FEBS Letters 355 (1994) 140–146

FEBS 14766

Does the solid-state structure of endothelin-1 provide insights concerning the solution-state conformational equilibrium?

Gregory M. Lee, Chinpan Chen, Thomas M. Marschner, Niels H. Andersen*

Department of Chemistry, University of Washington, Mail Stop BG-10, Seattle, WA 98195, USA

Received 18 August 1994; revised version received 28 September 1994

Abstract Additional NMR data (local NOE ratios and chemical shifts) for endothelin-1 supporting the existence of a relatively regular helix initiated abruptly at Lys^9 (with Asp^8 as an N-cap) and extending in all cases to Cys^{15} (and in a frayed form to Asp^{18} in some analogs) is presented. The recent solid-state structure [Janes et al. (1994), Nature Struct. Biol. 1, 311–319], in contrast, places the helix in the extreme C-terminal section of the structure and the Lys^9–Tyr^{13} segment is not helical. The X-ray structure does not predict the NOEs or chemical shifts observed for endothelins in aqueous media containing polar organic co-solvents. An analysis of the chemical shift data for reporter groups indicates that the helical conformational preference of endothelins is not significantly altered by the addition of acetonitrile, acetic acid, or ethylene glycol. The validity of the analytic strategy is supported by results for both more rigid and less helical analogs. We conclude that the structure observed in crystals obtained from purely aqueous media is influenced by intermolecular interactions in the solid state and is not a significant contributor to the conformational equilibrium observed for monomeric ET-1.

Key words: Endothelin; Conformation, X-ray vs. NMR; Detection of helicity

1. Introduction

Endothelins are a family of 21 residue bisdisulfide peptides that includes the most potent endogenous vasoconstrictor known, ET-1 [1].

Structural and pharmacological studies of the endothelin family of peptides have been one of the most active areas of medicinal research over the last few years [2,3], the number of papers on this subject exceeds 2000 by now, but no consensus has been reached concerning the stereostructural features associated with binding at the different classes of ET receptors [4–6]. NMR spectroscopy and X-ray crystallography can provide detailed information on the solution- or solid-state structure, respectively, of proteins. Conformationally versatile medium-sized peptides, such as endothelins, are not as well suited for either technique: (i) crystallization is more difficult and intermolecular contacts in crystals with low water content can influence the structural preference of a peptide which lacks intramolecular interactions that maintain a single stable structure, (ii) conformational versatility (producing multiple populated conformers with 20 ns–100 μs lifetimes) and the possibility of more rapid motional averaging can be a grave complication in NOE (nuclear Overhauser effect)-based structure elucidation. NMR structures have been reported for most members of the endothelin family; in many cases the species have been studied in both DMSO (a highly denaturing solvent) and in acidic aqueous media with varying quantities of solubilizing organic co-solvents added in order to support NMR concentrations without producing aggregates [7–9]. The earlier structural proposals [10–13] based on data for DMSO solutions have been largely discounted; more recent studies [9,14,15] indicate a complex conformational mixture is present in DMSO-containing media. The consensus feature of the NMR structures for mixed aqueous media is a somewhat irregular α-helix spanning from Lys^9 to at least Cys^{15}. A C-terminal extension to Leu^{17} has been reported [16] based on a preliminary analysis of NMR data for a more rigid analog, [$Pen^{3,15}$,Nle^7]ET-1 (henceforth bisPenET), which is an ET_A-selective agonist. A β-turn encompassing residues 5–8 has been reported in a number of studies [7,9,17–19]. The orientation of the C-terminus (residues 16→21) relative to the bicyclic core and the extent to which conformational averaging is occurring in that segment remains controversial. An X-ray crystal structure has recently been reported for ET-1 [20]; in decided contrast to the NMR structures, it displays a regular helical structure in the C-terminal fragment and the region from Lys^9 to Tyr^{13} does not display helical backbone torsion angles. The authors argue that the differences arise either because the NMR data were obtained in the presence of organic co-solvents or due to inherent problems in the protocols used for deriving NOE-based structure ensembles. Distance constrained dynamics programs can, indeed, be faulted for their inherent assumption that a single family of similar structures can fit all of the NOE data when fast dynamics and/or a conformational equilibrium are present. Notably, a string of i/i + 3 constraints (even if they are due to transiently formed helical turns in a conformational mixture) will produce a helical structure by such protocols. Lacking an r^{-6} dependence, chemical shifts are linear population-weighted averages over a conformational ensemble; chemical shift index (CSI) analyses [16,21] may, thus, be a better method for conformational mixtures. Herein we: (i) review the literature chemical shift data for endothelins, (ii) provide an extensive new body of experimental data for ET-1 and some analogs in a variety of media, (iii) examine other NMR diagnostics for helical structuring that do not rely on distance-constrained dynamics for structural conclusions, (iv) report the NOE-derived structure of a more rigid (and helical) ET-1 agonist, and (v) point out key NMR observations that cannot be explained by the X-ray structure. In sum, the X-ray structure is a poor model for rationalizing the solution state NMR data.

*Corresponding author. Fax: (1) (206) 685-8665.
E-mail: andersen@macmail.chem.washington.edu

SSDI 0014-5793(94)01153-2

In our view, the published solid-state conformation can not be a significant contributor to the conformational equilibrium presented by monomeric ET-1 in the solution.

2. Materials and methods

2.1. CSI histograms from previously published NMR data

Chemical shift data reported in nine papers [7–9,13,15,16,18,19,22], and in the Ph.D. thesis of C. Chen (University of Washington, 1992) were re-examined for concordance with 2D spectral figures appearing in the same reports; a few minor typographic errors and misattributions were corrected. In the present study, the shifts are converted to chemical shift indices (CSI histograms) by subtracting 'random coil' reference shifts from the reported or corrected values. (For mixed aqueous media, the Hα random coil reference values which we employ are, with the exception of Ile (4.10), Leu (4.28) and Val (4.05), 0.025 ± 0.031 ppm upfield of those reported by Wishart et al. [21]. The HN reference values are, with the exception of Asp (8.30) and Phe/Glu (8.23), narrowly centered about 8.14 ± 0.042 (S.E.M.). All current reference values will be provided upon request.) For DMSO data we use the published coil values [23].

2.2. Experimental methods

NMR spectra of [$Ala^{3,11}$,Nle^{7}]ET-1, [$Ala^{3,11,17}$,Nle^{7}]ET-1, [$Pen^{3,11}$, Nle^{7}]ET-1 (bisPenET, obtained from Dr. J.T. Hunt, Bristol-Myers Squibb), 20N-Me-bisPenET (also obtained from Dr. Hunt) and native ET-1 (Penninsula Labs, Belmont, CA) were recorded at 500 MHz in a variety of acidified (TFA or HOAc/HCO_2H) media, nominal pH 3.2–4.2. 2D spectra (NOESY, TOCSY and COSY) were recorded and processed using FELIX (Hare Research Inc.) as previously described [9,24]. Complete sequence-specific assignments were readily obtained using the now standard spin-system/sequencing (TOCSY/NOESY) methods of protein NMR [25].

2.3 Computational methods

Models of ET-1 and bisPenET were obtained by constrained dynamics simulated annealing (XPLOR3.1; Polygen/Molecular Simulations), including a standard Lennard–Jones potential rather than a purely repulsive van der Waals potential. Exaggerated bond length, angle and improper torsional potentials were employed in order to maintain standard geometries. In generating specific helical models, ϕ and ψ dihedrals were constrained in narrow ranges (± 10°) and the NOE force constant (k_{NOE}) was decreased so that the E_{NOE} contribution to E_{TOTAL} was less than the term for the constrained dihedrals. The previously published [9] distance constraints for ET-1 were employed; those employed for bisPenET will appear in a subsequent detailed account of the NMR work on a series of bisPen analogs. All computations were performed on Silicon Graphics Personal Iris 4D/25TG or Indigo workstations.

3. Results and discussion

The major discrepancies between the X-ray structure [20] of ET-1 and NMR-derived models [7–9,15,18] are most readily apparent upon examining key intermediate-range NOEs. An extensive web of i/i+3 NOEs appears from residues 9 through 16 in all published NMR studies in mixed aqueous media. Such NOE connectivities are particularly dense and tight between Lys^{9} and Val^{12} and these are not notably co-solvent dependent; for ET-3 at pH 3.6 in the absence of co-solvents, Mills et al. [22] report seven through-space contacts between these two key residues, all presumably ≤4.5 Å. Pertinent NOE distance constraints used to derive the structure of ET-1 in aqueous ethylene glycol [9] are given in Table 1. Although the coordinates for the X-ray structure have not been published, minimum values for these distances (see Table 1) can be measured, or deduced, from digitized images of the structural stereograms in the paper [20]. The X-ray structure fails to predict many quite strong NOEs in the N-terminal portion of the helix. In other cases, the X-ray structure predicts very strong NOEs where much smaller ones are observed in the NOESY data for the solution state species.

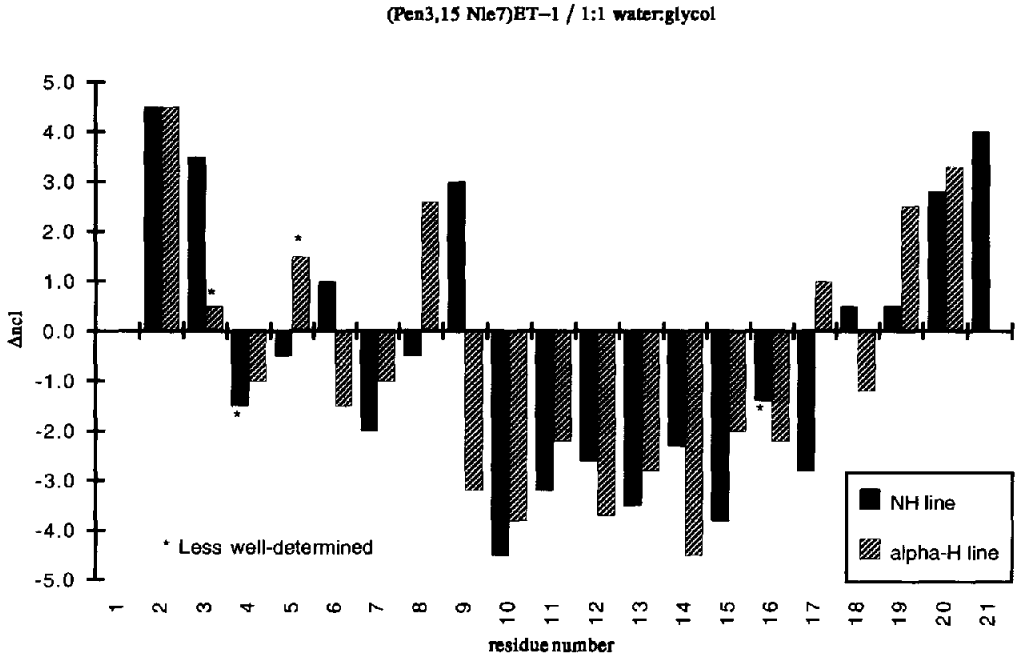

Fig. 1. Inter/intra-residue Hα/HN NOE ratios for bisPenET in 50% aq. ethylene glycol at 298 K. The Δncl value is the difference in the number of contour levels observed for inter- vs. intra-residue NOEs at each HN and Hα chemical shift line using a contour level multiplier of 1.4. The values thus correspond to $\log_{1.4}$[inter-NOE/intra-NOE] with positive values indicating the increasing contribution of extended chain conformations at that site. For each residue the measure for the HN line (NOE to α_{i-1} vs. α_i, predominantly reflecting ψ_{i-1}) appears before the measure at the Hα line (NOE to N_{i+1} vs. N_i, reflecting ψ_i). The values expected for a fully disordered and a 100% helical segment are +1.6 and −4.5 ± 0.6, respectively; the distances in a standard β-sheet conformation would yield a value of +4.3.

The comparisons in Table 1 argue that the X-ray structure cannot be *the* dominant solution state conformer.

Janes et al. suggest that the organic co-solvents used in NMR studies may have altered the conformational preference of ET-1 significantly. In the following sections we take up this point by using other NMR diagnostics and by ascertaining whether endothelins could have a rigid low energy conformation that includes a regular helix from residues 9 through 16.

3.1. *Other NMR data supporting a helical preference from Lys[9] to Cys[15]*

Previous NMR studies [16] have established that bisPenET (a potent agonist) is more helical than native ET-1, for example the exchange half-lives of the backbone NHs from residues 12–15 are ≥10 h under conditions where the most persistent NHs (residues 12–14) of native ET-1 have $t_{1/2}$ values of 1–3 h. The increased helicity is also evident by CD [26,27] and by a complete uninterrupted set of both α_iN_{i+3} *and* $\alpha_i\beta_{i+3}$ connectivities spanning from residue 9 to 17 [16]. Elimination of the 3,11-disulfide linkage greatly reduces vasoconstrictor activity [26,27,29,30] *and* net helicity as measured by CD [28–30].

Local NOE ratios provide a sensitive and unambiguous measure of backbone torsion angle distributions. Bradley et al. [31] validated an equation for deriving local fractional helicity from $N_iN_{i+1}/\alpha_iN_{i+1}$ NOE ratios; we have extended the method to $\alpha_iN_i/\alpha_{i-1}N_i$ and $\alpha_iN_i/\alpha_iN_{i+1}$ ratios [16]. Fig. 1 shows the inter/intra-residue Hα/HN NOE ratios for bisPenET in 50% aqueous glycol. The residue-by-residue contributions of local extended conformations are judged to be uniformly less than 15% from Lys[9] to Cys[15], with helicity estimates approaching 100% at several loci. Helicity estimates for residues 16–18 decrease but remain in excess of 40%. A similar plot for native ET-1 shows the same features from residue 2 through 15 but the contribution of extended conformations in the helical portion of that span is judged to be somewhat greater, perhaps as much as 25%. Beyond Cys[15], all of the Δncl values for native ET-1 are equal to or greater than +0.5, indicating less helicity in the C-terminal portion of the structure.

Chemical shift is very sensitive to the spatial disposition of hydrogens relative to π systems including the amide function; as a result, chemical shifts change dramatically with alterations in backbone conformation. It is now well established that local helical preferences produce upfield shifts for the α-methine proton resonance [21,32,33]. Histograms of αCSIs over a helical span of a peptide typically reach values of −0.4 ppm at the center of the helix with smaller upfield shifts at the frayed ends. Fig. 2 collects αCSI and HN-CSI histograms for endothelins in aqueous glycol and aqueous acetic acid. The HN-CSI plots are included since HN shifts yield even larger deviations as peptide segments go from a disordered to an ordered state. (The direction of HN shift deviations is largely dependent on H-bonding and coulombic interactions and cannot be correlated with an α or β conformational preference.)

Fig. 2A shows the CSI histograms derived from our data for native ET-1, the more persistently structured bisPen analog and a more flexible [Ala[3,11]] analog. The Hα CSI histogram of the bisPenET analog reveals a more extensive (and presumably, less dynamic) helical conformation, while that for the 1,15-monodisulfide shows increased contributions by more extended local conformations in the 'helical' span. For bisPenET, the comparison of the data with and without added hexafluoroisopropanol shows that the increased helicity in the fluoroalcohol-containing medium reflects propagation further into the C-terminal fragment. An examination of the Hα and HN-CSI profiles in the Cys[3]→Asp[8] loop for this series of compounds indicates that the increased helix predominance from residue 9→15 is coupled to a structuring transition in the loop region. Since bisPenET is more rigidly structured and still retains full agonist activity, we view structures generated from NMR data for this analog as a superior model for the bioactive conformation of endothelins.

Published studies from other laboratories provide additional insights into the helical domain of endothelins: Dalgarno et al. [18] compared ET-1 with M7A and D8A mutants in 40% aq. acetic acid; Coles et al. [19] have reported shift data for a 3,11-monodisulfide, [(α-aminobutyric acid)[1,15]]ET-1, in 10% acetonitrile. Fig. 2B re-states the literature data as CSI histograms. Coles et al. concluded, based on NOE-constrained simulated annealing calculations (XPLOR3.0), that the conformation in the helical span was the same as that we reported for ET-1; however, the α-CSI plot suggests that the elimination of the 1,15-disulfide increases the contribution of local extended conformations throughout the helical region, and eliminates the large downfield shift at 15-HN. The data of Dalgarno et al. clearly reveal that the Asp[8]→Ala[8] substitution reduces the αH upfield shifts in the helical span, and also moderates all deviations from random coil values in the Ser[4]→Leu[6] portion of the loop region: precisely as seen in the more flexible mono-disulfide structures. We suggest that this is strong evidence for a helix N-capping role for Asp[8] and that this structural feature should be included in models of the solution-state conformation of endothelins. Although the pivotal position of Asp[8] was noted by Dalgarno et al., the specific N-capping role was not proposed.

3.2. *Is the helical preference from Lys[9] to Cys[15] medium dependent?*

We employ 9Hα, 12Hα, and 14Hα as reporter groups to ascertain the extent to which the organic co-solvents used in NMR studies influence helical preferences in this region. At the top of Table 2, the data for two bisPen analogs and a more flexible [Ala[3,11]] analog are given. In the central portion of Table 2, data for ET-1 in different mixed aqueous media are presented. The solvent mixtures are listed in order of increasing lipophilicity as judged by the chemical shift of the Ile[19]-γ_2 resonance*. Based on the reporter group shifts, the helix in native ET-1 is slightly less populated than in the bisPen analogs. The shift data also indicate that the polar organic solvents used for NMR investigations do not alter the fractional helicity significantly. Glycol addition produces a slight increase in helicity based on this analysis and this has been confirmed by CD studies [9,26,27]. A more detailed analysis of the helix-indicat-

*In increasingly lipophobic media, the Ile[19]-γ_2 resonance appears upfield due to shielding by the Trp[21] indole ring. The experimental evidence for this C-terminal structuring feature, which is present in all endothelins examined to date and in fragments (such as HLDIIW, AcCHLDIIW and VYFAHLDIIW) lacking the disulfide-linked core of natural endothelins, will be presented elsewhere. The effect of increasing interaction of the indole ring and the fatty side chain is reminiscent of the observed shift changes in the cyclic pentapeptide ET antagonist BQ-123, where a Leu-γ proton appears nearly 1 ppm upfield from its random coil value in media of high water content [34].

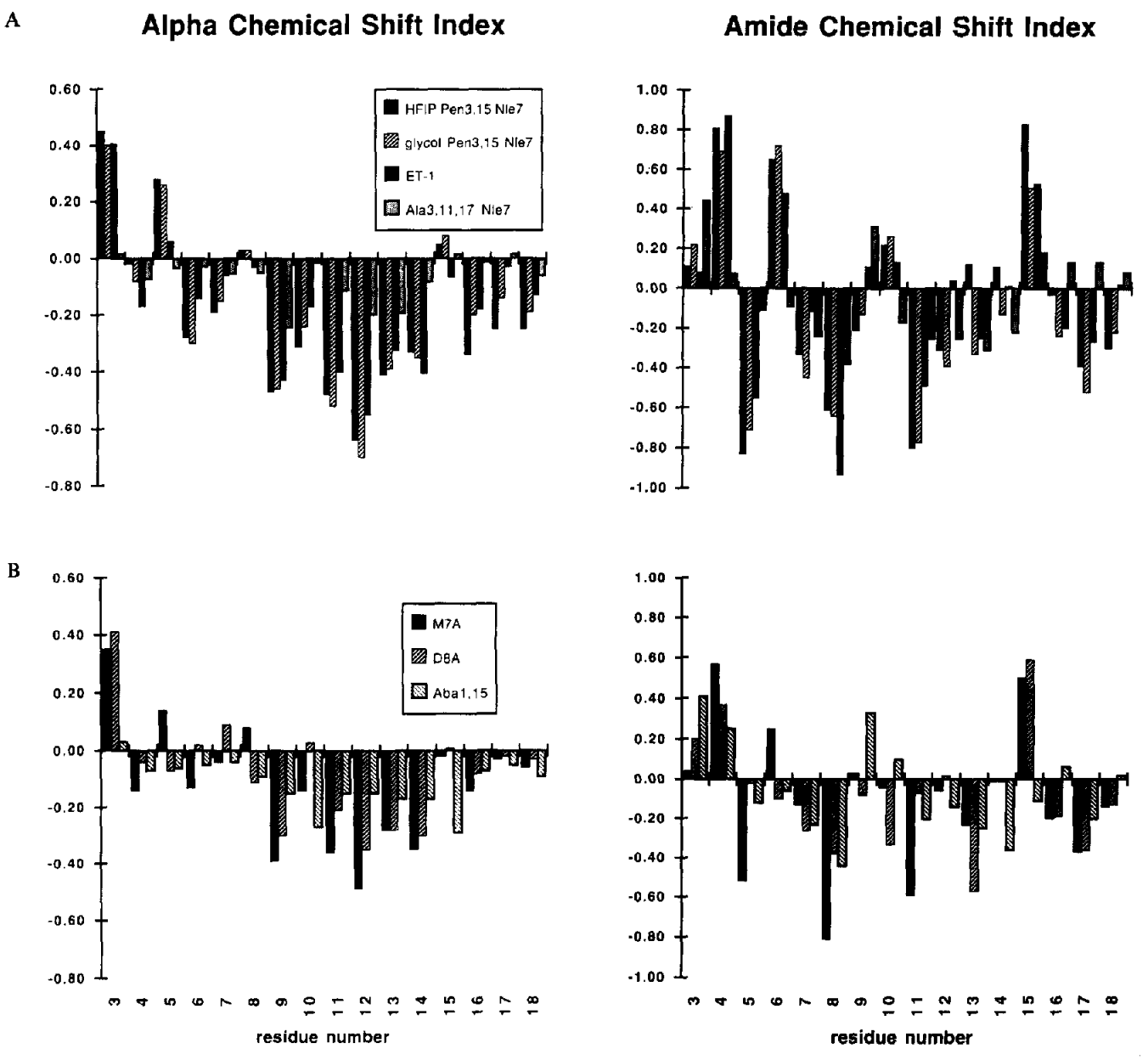

Fig. 2. CSI histograms for endothelins from residue 3 through 18; the C-terminal residues were excluded from these plots since the deviations were small and essentially the same for all of these species and for C-terminal fragments lacking the disulfide-linked endothelin core structure. (A) Hα (to the left) and HN-CSI plots vs. residue number for (left-to-right at each residue number) bisPenET (black bars, in 14% HFIP, 43% ethylene glycol, 43% H_2O, pH 3.5, 292 K; hatched bars, 50% ethylene glycol, pH 3.5, 298 K), native ET-1 (black bars, 60% ethylene glycol, pH 3.2, 307 K) and [$Ala^{3,11,17}$,Nle^{7}]ET-1 (grey bars, 65% ethylene glycol, pH 4.2, 305 K). HN chemical shifts have been corrected to 298 K based on the measured temperature gradients. All reference δ values for Hα have been increased by 0.04 ppm for the HFIP-containing medium, reflecting measured HFIP bulk solvent effects on shifts of structured proteins and fully disordered peptides examined in this laboratory. (B) CSI histograms for (left-to-right at each residue number) [Ala^{7}]ET-1 and [Ala^{8}]ET-1 (both in 40% acetic acid, 298 K), and [$Aba^{1,15}$]ET-1 (50% acetonitrile, 1.5% acetic acid, 298 K) based on the literature chemical shift data [18,19].

ing upfield Hα shifts, including the small effects of the added co-solvents upon the random coil reference values, indicates that 50+% acetonitrile and 40% acetic acid actually decrease the helix population slightly.

Conformational changes produced by the addition of the polar organic solvents to water for NMR studies do not appear to provide a rationale for the discrepancies between the NMR structures and the X-ray structure. In distinct contrast, the data for DMSO solutions reveal substantial disruption of the helix; but even in this highly denaturing solvent, upfield α chemical shift deviations are observed at Lys^{9} and Val^{12}, indicating significant local α conformational preferences are still present.

3.3. *Why is the helix from Lys^{9} to Cys^{15} not found in the solid-state structure of ET-1?*

Several explanations can be offered. For one, it could be

Table 1
NMR-detected intermediate range contacts absent in the X-ray structure

Connectivity	NOE distance constraint [9] (Å)	X-ray structure distance (Å)
From the helical region		
9 HA/12 HB	2.4–2.75	>8
9 HA/12 HG2*	2.55–3.25	>7.5
9 HA/12 HG1*	3.2–4.4	>9
9 HA/12 HN	2.9–3.7	>6
9 HA/13 HN	3.65–5.5	>8
10 HA/13 HN	3.2–3.7	>5.5
10 HA/13 HB*	2.9–3.65	≥5
10 HA/14 HN	3.55–4.35	>6.5
11 HA/14 HN	3.2–4.8	>5.5
12 HA/17 HN	3.2–3.8	⩾5
13 HA/15 HN	3.5–4.6	>5.5
13 HA/16 HN	3.35–3.9	>6
From other regions		
5 HN/11 HB*	3.1–3.9	>5.5
5 HB*/7 HN	3.2–4.25	>6
6 HA/12 HG2*	2.6–3.5	>8
12 HG1*/16 HD2	3.0–4.0	>7.5
19 HA/20 HN	2.05–2.55	>3.2
19HG2*/21 HN	3.35–4.75	>6.5
Close contacts predicted by the X-ray structure		
12 HA/14 HN	3.6–4.7	<2.5
12 HA/13 HN	3.3–3.65	⩽2.4
13 HN/14 HN	2.75–3.11	<1.9
6 HA/7 HN	2.8–3.45	<2.3

An asterisk following a proton label indicates a wildcarded set of equivalent, shift coincident, or stereochemically unassigned prochiral hydrogens. The distances reported correspond to an $<r^{-6}>$ average is such instances.

argued that a regular α helix from Lys[9] to Cys[15] is not a stable conformation; that the steric and covalent constraints of native ET-1 and bisPenET preclude this as an energy well structure. If this were the case, the NMR data could reflect a 'dynamic helix' in which a non-helical segment appears at different loci in the resulting solution-state conformational mixture and one of these less helical forms could be that observed in the solid state. Alternatively, the solid-state structure may be the result of interactions that are not present in the monomeric solution-state conformational mixture. We have probed this question by comparing NOE constraint violations and constraint-induced structural distortions for parallel simulated annealing runs with and without torsion constraints that enforce a regular helical geometry from Lys[9] to His[16]. The backbone torsion angles that result for bisPenET from the two simulations appear in Fig. 3. We selected this more rigid analog for the illustration since the added geminal dimethyl groups present make it the species most likely to show steric interactions that preclude certain regions of conformational space. Comparable results were obtained with native ET-1 (data not shown); however, the structure derivation with heavily weighted NOE constraints produces greater backbone torsion variability at residues 15 and 16.

In order to draw conclusions concerning the relative structure-distorting effects of NOE constraints vs. helical torsion angles, the force constants for the NOE and constrained dihedral potentials were adjusted so as to yield the same net constraint contribution (82 ± 12 kcal/mol) to E_{TOTAL}. In the protocol enforcing helical geometries (ϕ/ψ, ±< 10°), the E_{NOE} term represented only 33 ± 2% of the total constraint contribution to E_{TOTAL}; in the structure derivation with a reduced k_{cdih} term, the E_{NOE} term contributed fully 90 ± 6% of the constraint con-

Table 2
Ile[19]-γ_2 and helix reporter group chemical shifts

Lys-α	Val-α; γ,γ′	Phe-α	19γ_2 shift	Conditions
Most helical				
3.84	3.37; 1.01, 0.81	4.30	0.28[b]	50% glycol, 298 K, 20NMe-bisPenET[a]
3.86	3.35; 1.02, 0.81	4.25	0.64[b]	50% glycol, 298 K, bisPenET[c,d]
Less helical				
4.08	3.85; 0.86, 0.76	4.52	0.62	65% glycol, 305 K, [Ala[3,11,17],Nle[7]] ET-1[a]
Media effects, mixed aqueous conditions				
3.92	3.54; 1.02, 0.89	4.21	0.51	10% CD_3CO_2H, 293 K, [7]
(4.00	3.74; 0.86, 0.80)[e]	n.a.	0.52	H_2O, 303 K, [22] (ET-3)
3.90	3.49; 0.99, 0.840	4.23	0.53	40% glycol, 295 K[a]
3.89	3.50; 0.975, 0.835	4.195	0.605	60% glycol, 307 K[c]
3.91	3.59; 0.97, 0.84	4.27	0.61	30% CD_3CN, 303 K, [8]
3.95	3.58; 1.02, 0.89	4.28	0.62	40% CD_3CO_2H, 298 K, [18]
3.94	3.51; 0.97, 0.83	4.27	0.63	75% glycol, 305 K[a]
3.85	3.52; 0.94, 0.81	4.20	0.67	50% CD_3CN, 298 K, [15] [Nle[7]]
3.895	3.59; 0.93, 0.80	4.25	0.695	80% CD_3CN, 303 K[a]
DMSO media				
3.94	3.85; 0.80, 0.74	4.40	0.73–0.75	90–100% DMSO, 295–310 K[d,f]
4.06	3.99; 0.76, 0.71	4.52	0.74	93% DMSO, 295 K, [Ala[3,11],Nle[7]]ET-1[a]
4.29	4.26; 0.98, 0.92	4.56	0.86	DMSO reference values

Aqueous reference values[a]: Lys-α, 4.33; Val-α γ, γ′, 4.05; 0.91, 0.75; Phe-α, 4.60; Ile-γ_2, 0.77.
[a]Previously unreported data from this laboratory.
[b]This dramatic change in chemical shift for Ile-γ_2 remains unexplained. The 20N-Me analog is an ET_A receptor-selective antagonist (unpublished observations of J.T. Hunt at Bristol-Myers Squibb, Princeton, NJ).
[c]Published data from this laboratory [9,16].
[d]Data from this laboratory, previously reported in the Ph.D. thesis of C. Chen (University of Washington, 1992).
[e]Entirely comparable chemical shifts are not expected for ET-3 due to the local effects of nearby ET-1 to ET-3 residue substitutions – M7K, F14Y and possibly L6Y.
[f]These chemical shifts are in full accord with values previously reported for this medium [13,15].

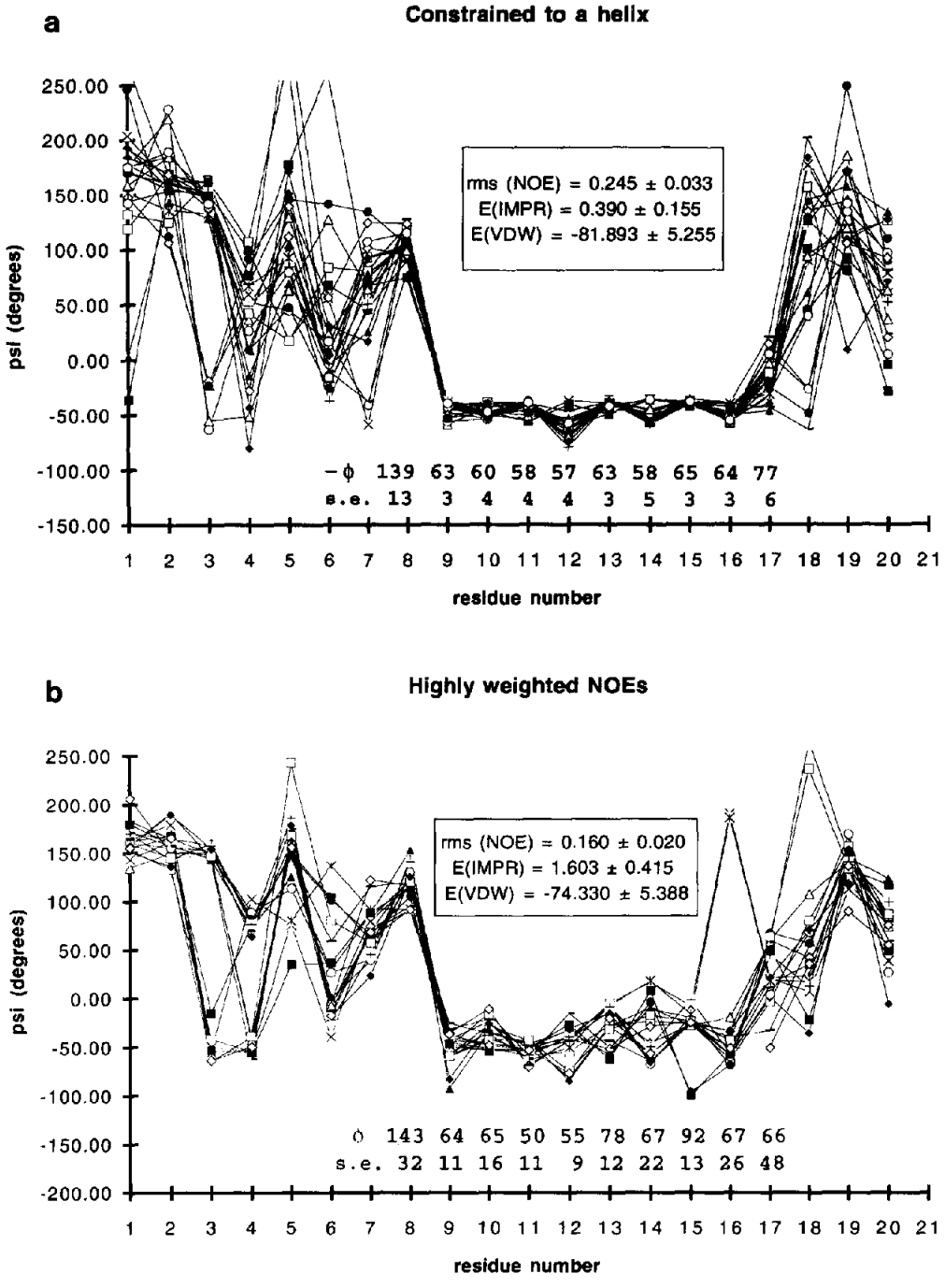

Fig. 3. Plots of ψ_i vs. residue number (i) for bisPenET models with varying relative weights for the NOE constraints and a set of torsion constraints forcing standard helical ϕ/ψ values from residue 9 to 16. Panel A shows the result for forcing torsion constraints, and panel B that for heavily weighted NOE constraints. The corresponding $[-\phi_i]$ values (and ±S.E.M.) are shown below each trace for the helical domain. The ensemble average (and ±S.E.M.) values of NOE distance rms violation, E_{IMPR} and E_{VDW} are inserted for each ensemble. For panel A the wide variance in ψ_i (and ϕ_i, not shown) values for the $Cys^3 \rightarrow Nle^7$ indicates that several unstrained conformers of the loop are compatible with a helical conformation from residue 9 to 16. In the plot for heavily-weighted NOEs, a consensus conformation is also apparent for the Ser^5–Asp^8 region.

tribution to E_{TOTAL}. Structural distortions caused by the constraints appeared exclusively in the E_{IMPR} and E_{VDW} terms, the angle and bond rms terms were identical and indicated no significant distortions from normal geometry (±2.5° and ±0.007 Å, respectively).

The increased NOE violation rms in the helical state model and the structural distortions that result when the k_{NOE} term is heavily weighted, indicate that some mutually inconsistent NOEs are observed due to residual dynamics in the solution state. The helical structures display less distortions than those produced when the k_{NOE} term is increased. Modeling thus suggests that endothelins could adopt a 'static' and quite regular

helical conformation. Clearly, another rationale is required in order to explain the conformational features for the Asp^8–Tyr^{13} segment in the X-ray structure.

The ET-1 crystals examined by X-ray were obtained from water with no added solvents, surfactants or buffers. It has been reported [35,36] that ET-1 aggregates in pure water at concentrations exceeding 22 μM. Janes et al. [20] note a 'dimer contact' which buries 800 Å^2 of surface area in the solid-state structure with the closest backbone–backbone distances at residues 12–13. An intermolecular H-bond, Tyr^{13}-OH→O = C-Asp^8 was also noted in that paper. The structural figures suggest that the fatty side chains of Val^{12} and Met^7 could also be in the contact region of the dimer. We suggest that crystallization from a medium in which the peptide is present as an aggregate has resulted in a dimer structure in which an intermolecular hydrophobic cluster has provided sufficient stabilization to overcome the helical propensity of the $Lys^9 \rightarrow Tyr^{13}$ span in the monomeric state. As a result, the X-ray structure of ET-1 is a poor model for the solution state conformational mixture. The short proton–proton distances found in the crystal structure, which are not confirmed by NOEs in the solution state, suggest that the solid-state conformer is not significantly populated in the solution state conformational equilibrium of endothelin monomers.

In summary, the NMR data given herein indicate that intact monomeric endothelins have a substantial helical conformation preference from Lys^9 to Cys^{15} which can partially propagate into the nearby portion of the C-terminal appendage. As the helical span gains stability and structural regularity, a single (but still not fully defined) structure dominates increasingly in the residue 4→8 loop region. The consensus structure for this loop [$\phi_6 = -85 \pm 17$, $\psi_6 = -1 \pm 19$, $\phi_7 = -76 \pm 18$, $\psi_7 = 63 \pm 19$] evident in Fig. 3B bears some resemblance to a type I β-turn. NMR data also indicate that the conformational equilibrium for the extreme C-terminus ($Asp^{18} \rightarrow Trp^{21}$) in the solution state is not influenced by its attachment to the bisdisulfide-linked core. It remains to be determined how relevant these solution-state structural features are to endothelin pharmacology.

Acknowledgements: This work was supported by a grant from the Bristol-Myers Squibb Institute for Pharmaceutical Research.

References

[1] Yanagisawa, M., Kurihara, H., Kimura, S., Tomobe, Y., Kobayashi, M., Mitsui, Y., Yazaki, Y., Goto, K. and Makaki, T. (1988) Nature 332, 411–415.
[2] Doherty, A. M. (1992) J. Med. Chem. 35, 1493–1508.
[3] Abstracts of the International Business Communications USA Symposium, Endothelin Inhibitors, Advances in Therapeutic Applications and Development, 9–10 June 1994 Philadelphia, PA.
[4] Arai, H., Hori, S., Aramori, I., Ohkubo, H. and Nakanashi, S. (1990) Nature 348, 730–732.
[5] Sakurai, T., Yanagisawa, M., Takuwa, Y., Miyazaki, H., Kimura, S., Goto, K. and Masaki, T. (1990) Nature 348, 732–735.
[6] Karne, S., Jayawickreme, C.K. and Lerner, M.R. (1993) J. Biol. Chem. 268, 19126–19133.
[7] Tamaoki, H., Kobayashi, Y., Nishimura, S., Ohkubo, T., Kyogoku, Y., Nakajima, K., Kumagaye, S.-i., Kimura, T. and Sakakibara, S. (1991) Protein Eng. 4, 509–518.
[8] Reily, M.D. and Dunbar Jr., J.B. (1991) Biochem. Biophys. Res. Commun. 178, 570–577.
[9] Andersen, N.H., Chen, C., Marschner, T.M., Krystek Jr., S.R. and Bassolino, D.A. (1992) Biochemistry 31, 1280–1295.
[10] Saudek, V., Hoflack, J. and Pelton, J.T. (1989) FEBS Lett. 257, 145–148.
[11] Endo, S., Inooka, H., Ishibashi, Y., Kitada, C., Mizuta, E. and Fujino, M. (1989) FEBS Lett. 257, 149–154.
[12] Saudek, V., Hoflack, J. and Pelton, J. T. (1991) Int. J. Pept. Protein Res. 37, 174–179.
[13] Munro, S., Craik, D., McConville, C., Hall, J., Searle, M., Bicknell, W., Scanlon, D. and Chandler, W. (1991) FEBS Lett. 278, 9–13.
[14] Brown, S.C., Donlan, M.E. and Jeffs, P.W. (1990) in: Proceeding of the 11th American Peptide Symposium (Rivier, J.E. and Marshall, G.R., eds.) pp. 552–556, Pierce Chem. Co., Rockford, IL.
[15] Aumelas, A., Chiche, L., Mahe, E., Le-Nguyen, D., Sizun, P., Berthault, P. and Perly, B. (1991) Int. J. Peptide Protein Res. 37, 315–324.
[16] Andersen, N. H., Cao, B. and Chen C. (1992), Biochem. Biophys. Res. Commun. 184, 1008–1014.
[17] Krystek Jr., S.R., Bassolino, D.A., Novotny, J., Chen, C., Marschner, T.M. and Andersen, N.H. (1991) FEBS Lett. 281, 212–218.
[18] Dalgarno, D.C., Slater, L., Chackalamannil, S. and Senior, M.M. (1992) Int. J. Peptide Protein Res. 40, 515–523.
[19] Coles, M., Munro, S.L.A. and Craik, D.J. (1994) J. Med. Chem. 37, 656–664.
[20] Janes, R.W., Peapus, D.H. and Wallace, B.A. (1994) Nature Struct. Biol. 1, 311–319.
[21] Wishart, D.S., Sykes, B.D. and Richards, F.M. (1992) Biochemistry 31, 1647–1651.
[22] Mills, R.G., O'Donoghue, S.I., Smith, R. and King, G.F. (1992) Biochemistry 31, 5640–5645.
[23] Bundi, A., Grathwohl, C., Hochmann, J., Keller, R.G., Wagner, G. and Wüthrich, K. (1975) J. Magn. Reson. 18, 191–198.
[24] Andersen, N.H., Cao, B., Rodríguez-Romero, A. and Arreguin, B. (1993) Biochemistry 32, 1407–1422.
[25] Wüthrich, K. (1986) NMR of Proteins and Nucleic Acids, Wiley, New York.
[26] Harris, S.M. (1993) Ph.D. thesis, University of Washington, Seattle, USA.
[27] Andersen, N.H., Harris, S.M., Lee, V.G., Liu, E., C.-K., Moreland, S. and Hunt, J.T. (1994) Biorg. Med. Chem. (submitted).
[28] Pelton, J.T. and Miller, R.C. (1991) J. Pharm. Pharmacol. 43, 43–45.
[29] Hunt, J.T., Lee, V.G., Stein, P.D., Hedberg, A., Liu, E.C.-K., McMullen, D. and Moreland, S. (1991) Bio-Org. Medicinal Chem. Lett. 1, 33–38.
[30] Topouzis, S., Pelton, J.T. and Miller, R.C. (1989) Br. J. Pharmacol. 98, 669–677.
[31] Bradley, E.K., Thomason, J.F., Cohen, P.A. and Kuntz, I.D. (1990) J. Mol. Biol. 215, 607–622.
[32] Jiménez, M.A., Nieto, J.L., Herranz, J., Rico, M. and Santoro, J. (1987) FEBS Lett. 221, 320–324.
[33] Szilágyi, L. and Jardetzky, O. (1989) J. Magn. Reson. 83, 441–449.
[34] Krystek Jr., S.R., Bassolino, D.A., Bruccoleri, R.E., Hunt, J.T., Porubcan, M.A., Wandler, C.F. and Andersen, N.H. (1992) FEBS Lett. 299, 255–261.
[35] Bennes, R., Calas, B., Chabrier, P.-E., Demaille, J. and Heitz, F. (1990) FEBS Lett 276, 21–24.
[36] Calas, B., Harricane, M.-C., Gulmard, L., Heitz, F., Mendre, C., Chabrier, P.E. and Bennes, R. (1992) Peptide Res. 5, 97–101.